Output coupling methods for cavity-based high-harmonic generation

Kevin D. Moll,* R. Jason Jones,† and Jun Ye

JILA, National Institute of Standards and Technology and University of Colorado
Boulder, CO 80309-0440
mollk@jila.colorado.edu

http://jilawww.colorado.edu/YeLabs

Abstract: We have investigated the coupling efficiency and cavity loss associated with a ring cavity that has a hole in one of the focusing mirrors. The aperture provides a means through which intracavity high-harmonic generation can be coupled from the cavity. By studying different cavity geometries and input modes we have found that the integration of phase-plates on the focusing mirrors provides the best performance in terms of input coupling efficiency, cavity loss, and output-coupling of the generated high harmonic light.

OCIS codes: (140.4780) Optical resonators, (140.7240) UV, XUV and X-ray lasers, (190.2620) Frequency conversion, (320.7110) Ultrafast nonlinear optics

References and links

1. M.J. Thorpe, K.D. Moll, R.J. Jones, B. Safdi, and J. Ye, "Broadband cavity ringdown spectroscopy for sensitive and rapid molecular detection," Science **311**, 1595 (2006).
2. M.J. Thorpe, R.J. Jones, K.D. Moll, J. Ye, and R. Lalezari, "Precise measurements of optical cavity dispersion and mirror coating properties via femtosecond combs," Opt. Express **13**, 882 (2005).
3. R.J. Jones and J. Ye, "High-repetition-rate coherent femtosecond pulse amplification with an external passive optical cavity," Opt. Lett. **29**, 2812 (2004).
4. V.P. Yanovsky and F.W. Wise, "Frequency doubling of 100-fs pulses with 50% efficiency by use of a resonant enhancement cavity," Opt. Lett. **19**, 1952 (1994).
5. F.O. Ilday and F.X. Kartner, "Cavity-enhanced optical parametric chirped-pulse amplification," Opt. Lett. **31**, 637 (2006).
6. R.J. Jones, K.D. Moll, M.J. Thorpe, and J. Ye, "Phase-coherent frequency combs in the EUV via high-harmonic generation inside a femtosecond enhancement cavity," Phys. Rev. Lett. **94**, 193201 (2005).
7. C. Gohle, *et al.*, "A frequency comb in the extreme ultraviolet," Nature **436**, 234 (2005).
8. K.D. Moll, R.J. Jones and J. Ye, "Nonlinear dynamics inside femtosecond enhancement cavities," Opt. Express **13**, 1672 (2005).
9. A. Siegman, *Lasers*, (University Science Books, Sausalito, California, 1986).
10. G.B. Arfken and H.J. Weber, *Mathematical methods for physicists, 4th ed.*, (Academic, San Diego, California, 1995).
11. J. Peatross, J.L. Chaloupka, and D.D. Meyerhofer, "High-order harmonic-generation with an annular laser-beam," Opt. Lett. **19**, 942 (1994).
12. E.W. Weisstein,"Generalized Hypergeometric Function." (MathWorld - A Wolfram Web Resource, 2006), http://mathworld.wolfram.com/GeneralizedHypergeometricFunction.html
13. S.V. Fomichev, P. Breger, B. Carre, P. Agostini, and D.F. Zaretsky, "Non-collinear high-harmonic generation," Laser Phys. **12**, 383 (2002).
14. S.V. Fomichev, P. Breger, and P. Agostini, "Far-field distribution of third-harmonic generation by two crossed beams," Appl. Phys. B **76**, 621 (2003).

#72214 - $15.00 USD Received 22 June 2006; revised 15 August 2006; accepted 16 August 2006

1. Introduction

Recent experiments in which broadband femtosecond combs are coupled to passive optical cavities have demonstrated great potential for new optical devices and measurement techniques. While some experiments utilize the increased frequency sensitivity of a cavity to more precisely measure optical parameters such as absorption [1] and group-delay dispersion [2] over a broad bandwidth, other experiments make use of the pulse-energy enhancement inherent to the cavity to generate more intense sources [3] and enhance nonlinear interactions [4, 5]. One particularly interesting experiment is the recent demonstration of generating a high repetition rate vacuum- and extreme-ultraviolet (VUV/XUV) source by coupling the light from a Ti:sapphire oscillator to a passive cavity [6, 7]. However, coupling the generated radiation out of the cavity presents many challenges. In this paper, we explore possible output-coupling methods to efficiently extract the high-harmonic radiation from the cavity.

The recent experimental demonstrations of cavity-based high-harmonic generation (HHG) utilized an intracavity sapphire plate oriented at Brewster's angle to couple the HHG from the cavity. A small Fresnel reflection occurs for the HHG because the sapphire plate is dispersive. However, this method has may limitations. For instance, the sapphire plate can limit the cavity energy enhancement. In order to reach the necessary intensities to achieve HHG with a cavity-enhanced technique, several conditions must be satisfied. First, the cavity must be low loss over the spectral bandwidth of the femtosecond laser. Because the sapphire plate must be placed near the intracavity focus, the entire spatial profile of the diffracting beam cannot be aligned at Brewster's angle. This additional loss limits the finesse that can be achieved. A second condition is that each component of the femtosecond comb must overlap a corresponding cavity mode. This requires that the cavity dispersion must be minimized such that the free spectral range of the cavity is uniform as a function of wavelength. In order to compensate the dispersion of the sapphire plate, a negative group-delay dispersion (NGDD) mirror must be utilized. However, NGDD mirrors are not ideal for low-loss/broadband because of the increased number of coating layers. Additionally, compensating for higher-order dispersive terms of the sapphire can be problematic.

A second limitation of the intracavity plate based method of output coupling arises from the fact that the sapphire plate must be located near the intracavity focus in order to couple out the HHG before it hits another cavity mirror. For high-finesse cavities, the high intensities inside the plate lead to significant spectral distortions due to nonlinear processes in the plate [8] which reduce the ability to couple the entire comb to the cavity. A final limitation of the sapphire plate is that the output coupling efficiency is low. At low-order harmonics, the index of refraction of the sapphire has not changed sufficiently to lead to a large Fresnel reflection. At higher-order harmonics, the sapphire becomes absorbing, and even though the light is reflected from the front surface, absorption of the evanescent wave penetrating the sapphire leads to a maximum reflectivity of approximately 20 percent.

An alternative output coupling method, which will be the focus of this article, is to couple the HHG through a small hole in the concave mirror after the intracavity focus. By coupling a higher-order spatial beam to the cavity, the pump beam will avoid the hole, maintaining the high finesse. However, the HHG generated at the focus will diffract at a smaller angle due to its decreased wavelength and will partially couple through the hole. This technique eliminates many of the problems associated with the sapphire plate. An additional technique that we will briefly discuss towards the end of this paper is a noncollinear geometry in which the HHG is generated by two intracavity pulses intersecting at a slight angle. This technique bears similarity to the first approach except that the two beams are separate instead of being derived from the two lobes of the higher-order spatial mode.

#72214 - $15.00 USD Received 22 June 2006; revised 15 August 2006; accepted 16 August 2006

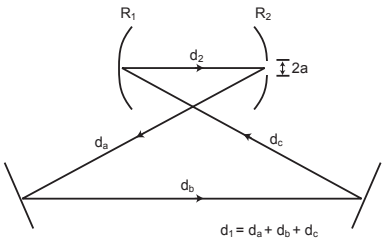

Fig. 1. Schematic of the ring cavity under investigation. A hole of radius a is drilled in one of the curved mirrors to allow the high-harmonic light to escape from the cavity. The curved mirrors have radius of curvature R_1 and R_2 and the distances of separation between the mirrors are denoted as d_i.

2. Computational method

In order to evaluate the performance of the proposed output-coupling scheme, the cavity loss introduced by the hole and the spatial profile of the HHG at the machined mirror must be calculated. Figure 1 depicts the cavity geometry we are investigating with the relevant dimensions labeled. While many methods exist for calculating the cavity modes (see for example, [9]), many of these techniques are specialized to calculating the laser-cavity mode that experiences the most gain. In our case, however, we are seeking the cavity modes which are low-loss, but are also reasonably smooth and can be easily excited with a laser beam. The method we have chosen to calculate the cavity modes is to express the cavity mode as a superposition of the Laguerre-Gaussian modes of the unapertured cavity which form a complete basis [9]:

$$u_v(r,\phi) = \sum_{p=0}^{\infty} c_p \frac{2}{\sqrt{2\pi}} \sqrt{\frac{p!}{(p+v)!}} \frac{L_p^v(2\frac{r^2}{w^2})}{w} \left(\frac{\sqrt{2}r}{w}\right)^v e^{ik\frac{r^2}{R}} e^{-\frac{r^2}{w^2}} e^{-iv\phi} e^{i\psi_{p,v}} \tag{1}$$

where (r,ϕ) represent the radial and angular coordinates of the field amplitude u_v, v is the angular mode order number, and p is the radial mode order number. Physically, the weighting coefficient c_p represents the amount of the unapertured cavity mode with radial mode-order p that is contained in the physical cavity mode of the apertured cavity. R and w represent the position dependent radius of curvature and width of the unapertured modes inside the cavity and can be calculated with ABCD matrix techniques, $k = 2\pi/\lambda$ where λ is the laser wavelength, L_p^v is the associated Laguerre polynomial [10], and $\psi_{p,v}$ is the position dependent geometrical phase.

Using this representation, the weighting coefficients of the cavity mode can be solved for using matrix eigenvalue methods. The associated eigenvalue β, which encodes the round-trip cavity loss and longitudinal frequency, can be calculated by solving the matrix equation:

$$AD_2D_1\vec{c} = \beta\vec{c} \tag{2}$$

where $\vec{c}$ is a vector with elements c_p, and A is a matrix which is responsible for modeling the aperture by decomposing the field $u(r)$ before the mirror into a field which is zero for $r < a$ after the mirror. Diagonal matrices D_i account for the fact that different transverse modes accumulate different geometrical phase by traveling distance d_i in the cavity where (as shown in Fig. 1) we use d_1 to represent the overall path outside the two curved mirrors and d_2 for the distance between the two curved mirrors. Fortunately, the elements of the aperture matrix

$$A_{p,m} = \sqrt{\frac{p!}{(p+v)!}} \sqrt{\frac{m!}{(m+v)!}} S_{p,m}^{v,v} \tag{3}$$

#72214 - $15.00 USD Received 22 June 2006; revised 15 August 2006; accepted 16 August 2006

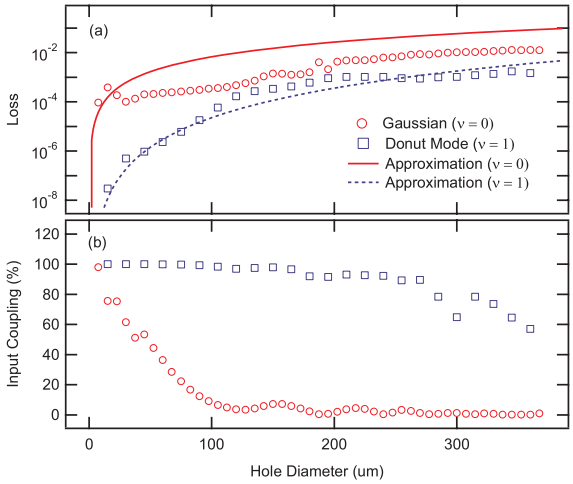

Fig. 2. (a) Comparison of expected cavity loss for a gaussian $(\nu = 0)$ and donut-mode $(\nu = 1)$ beam coupled to a cavity with a hole drilled in one of the mirrors. The losses were also approximated by integrating the power of the unperturbed beam over the hole area which are shown as solid and dashed lines for the Gaussian and donut mode, respectively. (b) Percentage of light that can be coupled to cavity mode using an ideal gaussian or donut-mode.

where

$$S^{\nu,\eta}_{p,m} = \int_{2a^2/w_0^2}^{\infty} L^{\nu}_{p}(y) L^{\nu}_{m}(y) y^{\eta} e^{-y} dy \tag{4}$$

can be easily calculated by making use of the recurrence relationship

$$S^{\nu,\eta}_{p,m} = L^{\nu}_{p}(y_0) L^{\nu}_{m}(y_0)(y_0)^{\eta} e^{-y_0} - \sum_{i=0}^{p-1} S^{\nu,\eta}_{i,m} - \sum_{j=0}^{m-1} S^{\nu,\eta}_{p,j} + \eta S^{\nu,\eta-1}_{p,m}. \tag{5}$$

where $y_0 = 2a^2/w_0^2$ and w_0 is the field 1/e half-width of the unapertured gaussian mode on the apertured mirror. The coefficient vector $\vec{c}$ is truncated at a finite number of terms, and β is solved by inverse iteration as the size of the aperture adiabatically increases.

3. Results

As a specific example to study, we have chosen cavity parameters similar to those used experimentally in Refs. [6, 7]. The curved mirrors have a radius of curvature $R_1 = R_2 = 10$ cm, the long arm of the cavity has length $d_1 = 2.9$ m and the short path of the cavity ($d_2 \approx 10$ cm) will be varied to probe the output-coupling scheme for different levels of cavity stability. In order to calculate the beam width of the cavity mode, a laser wavelength of $\lambda = 800$ nm was used.

Figure 2 compares the performance of the cavity when a gaussian beam ($\nu = 0$) and a donut-mode ($\nu = 1$) are coupled to a cavity in which d_2 is in the center of its stability region such that w = 860 μm. The expected round-trip cavity loss (Fig. 2(a)) is calculated as the hole size increases. As a comparison, a first-order approximation is also calculated in which the loss is computed by assuming the mode-profile does not change as the hole-size is increased and the loss is simply the fraction of the light that overlaps the hole. For the gaussian beam, the approximate expression overestimates the loss because the stable cavity mode for larger hole sizes reorganizes sufficiently to avoid the hole.

#72214 - $15.00 USD Received 22 June 2006; revised 15 August 2006; accepted 16 August 2006

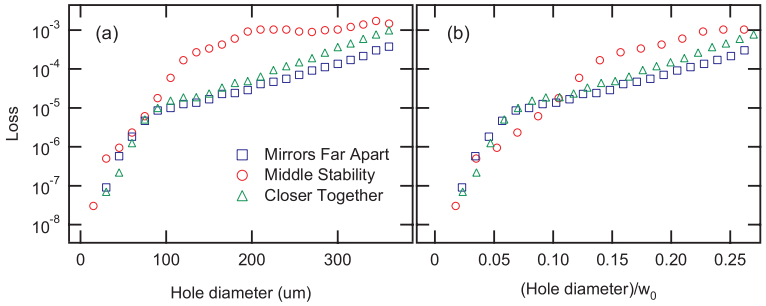

Fig. 3. (a) Comparison of loss for the donut mode at varying levels of cavity stability. (b) Fortunately, even after renormalizing the hole size by the mode diameter, for larger hole sizes the cavity loss is less when the cavity is operated near the edge of stability where the intracavity focus is tighter (△ and □).

Another issue that arises when comparing performance between the gaussian and donut mode is the input coupling efficiency. The reorganization of the gaussian beam that allows relatively low loss to be maintained leads to a dramatic reduction in the input-coupling efficiency (see Fig. 2(b)) since the cavity mode looks less like a gaussian. Large diffraction fringes also develop because the hard-edged aperture acts on the high-intensity portion of the gaussian beam. In contrast, high coupling efficiency can be maintained for the donut-mode at moderately large hole diameter.

The efficiency of HHG is very sensitive to the peak intensity of the laser pulse inside the gas sample being excited. As such, a tight intracavity focus is required. Besides changing the radius of curvature of the focusing mirrors, the intracavity focus can be made smaller by changing the mirror separation d_2 such that the cavity is operated near the edge of its stability regime. We have investigated the performance of the output coupling method as a function of the cavity stability. In Fig. 3(a), we present results of the calculated loss for the donut-mode when the cavity is operated at the center of its stability regime where the intracavity focus is 15-μm. In addition, we calculated the loss when the cavity is operated on either side of its stability regime such that the intracavity focus is 10-μm. The results of Fig. 3(a) can be misleading however because the mode size on the mirror increases as the focus is decreased. Thus, a smaller percentage of the light will impinge on the hole resulting in a smaller loss. However, the HHG will also be generated with a smaller transverse profile and will diffract more quickly. A fairer comparison can be made if the hole diameter is normalized by the mode diameter on the mirror. Figure 3(b) clearly shows that operating near the edge of cavity stability is advantageous both in terms of cavity loss and peak focal-intensity. The reduced loss experienced when the cavity is operated near the edge of stability when the fractional hole size is fixed can be understood by realizing that the curved mirrors form a perfect one-to-one telescope at both limits of cavity stability. This limiting case possesses lossless modes for any hole size.

While the donut mode offers better performance compared to the gaussian in terms of minimizing loss and improved input-coupling efficiency, there are several drawbacks. First, it is very difficult to achieve a donut mode directly from a mode locked laser. Second, the peak intensity at the focus for a donut mode is only $1/e \approx 37\%$ the peak intensity of the gaussian if the two beams have the same power. Considering the highly nonlinear nature of HHG, this reduction in peak intensity can lead to a significant reduction in the HHG yield. Third, slight astigmatism in the ring cavity breaks the longitudinal-mode degeneracy between the TEM_{01} and TEM_{10} modes. These difficulties can be partially addressed by inserting a phase-mask before the cavity which produces a beam with a gaussian intensity distribution but introduces a π phase shift

#72214 - $15.00 USD Received 22 June 2006; revised 15 August 2006; accepted 16 August 2006

between the two halves of the spatial profile. Computing the overlap integral of the beam with the TEM_{01} reveals that a conversion efficiency of 93% can be achieved. While a phase plate that increases ν by one could have been used, manufacturing a phase plate that creates a TEM_{01} is far simpler. In addition, the peak intensity of the TEM_{01} is twice that of the donut yielding only a 26% reduction in peak intensity relative to the gaussian. Since the TEM_{01} mode can be expressed as a superposition of the $\nu = \pm 1$ donut modes, the expected coupling efficiency and loss experienced by theTEM_{01} will be the same as that already calculated for the donut mode.

To experimentally verify the numerical results presented here, a phase plate was fabricated as well as mirrors with holes drilled in them. A 725-μm step was reactive ion etched onto a sapphire window which was inserted into the laser beam (with the step line cutting through the middle of the spatial profile) at Brewster's angle between the laser and enhancement cavity. This phase plate worked sufficiently well over the spectral bandwidth of $\sim$20 nm that could be coupled well into the cavity due to intracavity dispersion. With unapertured mirrors in the cavity, the coupling efficiency of the TEM_{01} mode was 85% of what could be achieved with the gaussian mode, compared to a theoretical limit of 93%. By filling the entire vacuum chamber with 1-Torr of Xenon, a strong plasma was observed indicating that sufficient peak intensity buildup in excess of 10^{13}W/cm^2 at the intracavity focus was still maintained with the TEM_{01} mode. An apertured mirror was then fabricated by mechanically counterboring a 3-mm hole into a glass substrate to within 1-mm of the reflecting surface. The remaining 1-mm was then laser machined to produce holes from 100 to 300 μm in diameter. The surface was then polished to the desired radius of curvature and coated with a high-reflector coating. When inserted into the cavity to which a TEM_{01} was coupled, a 100-μm hole changed the cavity finesse from 3300 to 2650 (as measured by cavity ringdown) corresponding to an additional 0.05% loss. This is comparable to that predicted by the simulations presented above. After coupling all aspects of the experiment together (input coupling efficiency, mode conversion, spectral filtering, hole loss), an intracavity pulse-energy enhancement of 275 was still experimentally achieved leading to visible ionization of Xenon at the intracavity focus.

A final drawback of not using a gaussian beam is that the HHG will not have a constant phase across its spatial profile because of the nonconstant phase of the fundamental beam. In addition, the harmonic will be generated in a ring (or dual lobed) which could lead to reduced output coupling since the peak intensity of the HHG will not be on-axis. In order to evaluate the output coupling efficiency, a simple model of HHG was used in which the cavity mode was calculated at the focus, raised to the *n*-th power where *n* was the harmonic order being investigated, and propagated to the mirror. Hence, the complicated intensity dependence and phase-matching aspect of HHG have been neglected. While this simple model should work well for approximating the spatial profile of the low-order harmonics, the absolute efficiencies at higher-order harmonic should be calculated using a more rigorous model for the HHG process. Figure 4 shows a comparison of the ninth-harmonic profiles at the apertured mirror for a gaussian, $\nu = 1$ donut, and TEM_{01} input modes when a 225-μm hole (shown as a white ring) is used. Even though the cavity loss for the $\nu = 1$ and TEM_{01} are identical, the output coupling through the aperture for the TEM_{01} is significantly higher. Whereas the phase of the ninth harmonic of the donut mode wraps 18π, resulting in a $\nu = 9$ character, the phase of the high-harmonic TEM_{01} simply contains a π phase step across the beam. This results in a predominantly $\nu = \pm 1$ character and a considerably smaller diffraction angle.

One solution that addresses these issues is to integrate $\lambda/2$ phase masks onto both concave mirrors of the cavity. In the long arm of the cavity, a TEM_{01} beam with low on-axis intensity is coupled to the cavity. Upon reflection from the concave mirror, the two lobes of the beam become in phase but retains a low-intensity on-axis. However, as the beam propagates to the focus, a strong on-axis intensity develops leading to strong axially-generated HHG [11]. Upon

#72214 - $15.00 USD Received 22 June 2006; revised 15 August 2006; accepted 16 August 2006

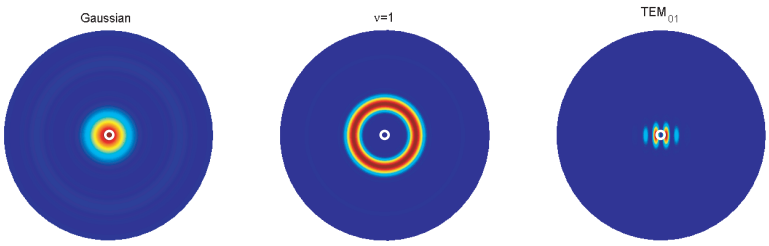

Fig. 4. Ninth-harmonic intensity profiles at the apertured mirror for gaussian, donut ($v = 1$), and TEM_{01} input beams. The high-harmonic donut has a $v = 9$ character. The white circle represent the 225-μm diameter aperture.

propagating to the apertured concave mirror, the fundamental beam redevelops the low-intensity node on-axis such that low loss is maintained. Finally, reflection from the apertured mirror with the integrated phase mask reproduces a TEM_{01} character to the beam.

Even though a TEM_{01} mode would be used in an actual experiment, it is easier to do the calculations in the basis of the donut mode. The action of a phase mask that maintains the intensity distribution but increases the azimuthal symmetry parameter, v, by one can be incorporated into the model as an additional transfer matrix, N, with components,

$$N_{q,p} = \int_0^\infty \frac{L_q^1(y)L_p^0(y)\sqrt{y}e^{-y}}{\sqrt{q+1}}dy = -\frac{\Gamma(p-\frac{1}{2})\Gamma(q+\frac{1}{2})_3F_2(-p,\frac{3}{2},-q;-q+\frac{1}{2},-p+\frac{3}{2};1)}{4\sqrt{\pi}\sqrt{q+1}\Gamma(p+1)\Gamma(q+1)} \tag{6}$$

where ${}_3F_2$ is the generalized hypergeometric function [12]. While calculating the matrix elements directly from Eq. 6 can be cumbersome for large p and q, a recurrence relationship can be derived to allow efficient computation of the matrix elements:

$$N_{q,p} = \frac{(-4q+8pq-7-8p^2+16p)}{2p(1+2q-2p)}N_{q,p-1} - \frac{(p-1)(5+2q-2p)}{p(1+2q-2p)}N_{q,p-2} \tag{7}$$

The loss resulting from the integration of a pair of phase masks on the two curved mirrors can therefore be computed by solving the matrix eigenvalue problem

$$\beta\vec{c} = AND_2N^TD_1\vec{c} \tag{8}$$

where the $v = 1$ beam is propagating in the d_1 arm of the cavity.

In order for the integrated phase plates to work effectively, the intensity distribution on the first focusing mirror must be reproduced on the second curved mirror. This is accomplished by operating near the edge of cavity stability such that the diffractive phase in propagating between the curved mirrors is about π radians for the gaussian mode of the unperturbed cavity. Figure 5 presents a comparison of the cavity loss for the gaussian and donut modes without the integrated phase masks and the hybrid mode resulting from the integrated phase masks. The cavity conditions correspond to the situation near the inner edge of stability in Fig. 3. As can be seen, the results for the hybrid mode matches well with the donut mode in terms of loss and coupling efficiency. Unlike the donut mode however, an intense on-axis distribution develops at the tight intracavity focus which will lead to improved harmonic generation and output coupling.

We have calculated the expected output coupling efficiency when a TEM_{01} mode is coupled to the cavity with and without the integrated phase masks. As shown in Fig. 6, the integrated phase plates lead to a dramatic increase in the output coupling, especially at lower order harmonics. Even for a relatively large hole of 250 μm, the loss can be maintained below 0.1% and

#72214 - $15.00 USD Received 22 June 2006; revised 15 August 2006; accepted 16 August 2006

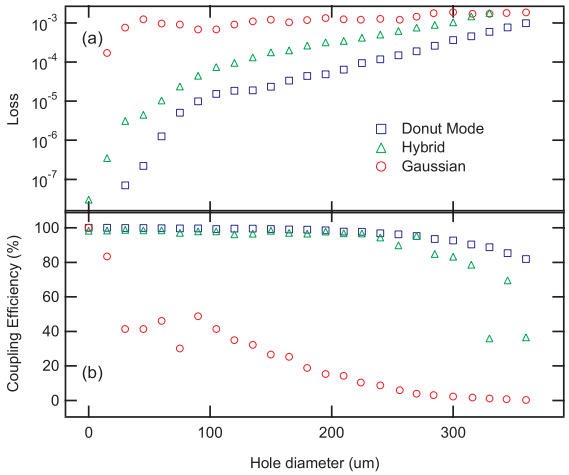

Fig. 5. (a) Intracavity loss near the inner edge of stability for a cavity that has phase masks integrated on the curved mirrors. A hybrid mode which has $v = 0$ and $v = 1$ character in different parts of the cavity is supported. For comparison, the round-trip loss without the integrated masks is also computed for an input gaussian and donut mode. (b) The hybrid mode can also be excited with similar coupling efficiency as the donut mode.

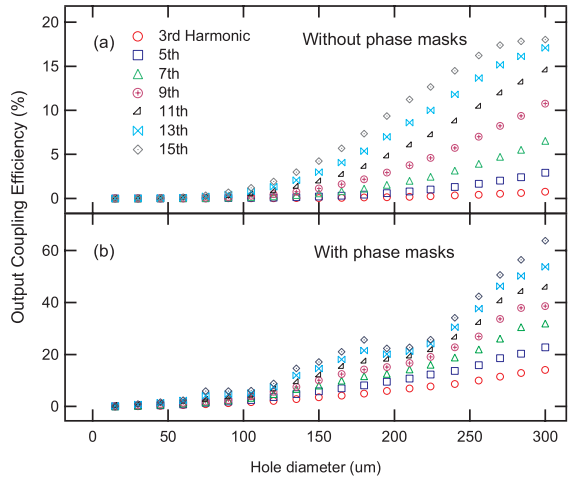

Fig. 6. Output coupling efficiency of the HHG for a cavity (a) without and (b) with phase masks integrated onto the concave mirrors. Note the vertical scale difference between (a) and (b)

an output coupling efficiency in excess of 40% at the fifteenth harmonic can be achieved. In addition, as stated above, HHG will be more efficiently generated because the peak intensity at the intracavity focus will be higher for the hybrid mode.

An additional output coupling method is to utilize a cavity that is twice as long as the laser cavity. As such, two pulses will be inside the buildup cavity. By using two sets of concave mirrors that share a common focus, HHG can be achieved in a noncollinear geometry [13, 14] and the high-harmonic light can escape through a small gap between the curved mirrors. (See Fig. 7). This method presents some advantages compared to the previously discussed

#72214 - $15.00 USD Received 22 June 2006; revised 15 August 2006; accepted 16 August 2006

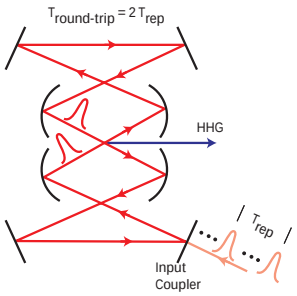

Fig. 7. Output coupling method using noncollinear geometry. The length of the optical cavity is twice the laser-cavity length such that two pulses inside the cavity can simultaneously focus into a gas sample. The noncollinearly generated HHG is output coupled through a gap between the two focusing mirrors.

schemes. First, separation of the high-harmonic from the fundamental light is simple because they are propagating in different directions. Second, no complicated fabrication is necessary. Finally, there is an inherent increase in the intensity at the focus by a factor of two since there are two separate pulses colliding. However, several disadvantages may lead to experimental challenges. First, since the cavity is twice as long, more mirrors would have to be used to fold the cavity into a reasonable size. This will increase the losses and dispersion and could limit the energy enhancement achieved. Second, the noncollinear geometry will limit the effective interaction length of the two pulses. Lastly, the cavity geometry must be arranged such that the two ultrashort pulses overlap in time at the focus. In addition, the two halves of the cavity need to be stabilized such that the two pulses will maintain constructive interference on axis.

4. Conclusion

Cavity enhanced HHG shows great promise for high-precision spectroscopy at vacuum ultraviolet wavelengths. In this paper we have presented several alternative geometries to help increase the fluence through more effective output coupling. While technically challenging to fabricate, the integration of phase masks onto the concave mirrors appears to be the most promising overall since a high finesse can be maintained, the cavity mode can be effectively excited, and a large percentage of the generated HHG can be coupled from the cavity.

Note added in proof: We have recently successfully coupled out the third harmonic through the aperture of the concave cavity mirror.

Acknowledgements

The authors would like to thank K. Čičak of NIST for fabrication of the phase mask to convert a gaussian into a TEM_{01} mode. We thank D. Yost, T. Schibli, and M. Thorpe for experimentally demonstrating output coupling of the third harmonic and M. Stowe for useful discussions. This work was supported by AFOSR and the MURI Program through the University of California at Berkeley. Partial support comes also from DARPA and NIST.

* Present address: Precision Photonics, Boulder, Colorado.
† Present address: Optical Science Center, University of Arizona, Tucson, Arizona.

#72214 - $15.00 USD Received 22 June 2006; revised 15 August 2006; accepted 16 August 2006